02

Computer simulation of nanoscopic phase-inhomogeneous states and phase diagrams of HTSC cuprates and nickelates

© A.S. Moskvin[1,2], Yu.D. Panov[1], V.A. Ulitko[1]

[1] Ural Federal University,
Yekaterinburg, Russia
[2] Institute of Metal Physics, Ural Branch, Russian Academy of Sciences,
Yekaterinburg, Russia

E-mail: alexander.moskvin@urfu.ru

More than 35 years of experience in the study of cuprate superconductors shows that the main characteristics of the phase diagram can only be obtained by taking into account mesoscopic static/dynamic phase inhomogeneity as a key property of these materials. Within a minimal model for the CuO_2/NiO_2 planes with the on-site Hilbert space reduced to only three effective valence centers $[CuO_4]^{7-,6-,5-}$ (nominally $Cu^{1+,2+,3+}$) with different conventional spin and different orbital symmetry we propose a unified non-BCS model that allows one to describe the main features of the phase diagrams of doped cuprates within the framework of a simple effective field theory. Using Maxwell's construction, the global nature of the electronic phase separation in the CuO_2 planes of HTSC cuprates is established, which makes it possible to understand and explain many fundamental features of the physics of the normal and superconducting state of cuprates, including the mechanism of formation of the HTSC and pseudogap phase. The features of phase-inhomogeneous states and their evolution with temperature and doping degree, including the special role of the impurity potential in cuprates/nickelates with nonisovalent substitution, are considered for particular examples of the charge triplet model in the framework of the classical Monte Carlo method.

Keywords: cuprates, nickelates, effective field theory, phase diagram, phase separation, Monte-Carlo.

DOI: 10.21883/PSS.2022.09.54148.09HH

1. Introduction

Today, there is no consensus on the theoretical model that allows one to describe the complete $T-x$ ($T-n$, $T-p$) phase diagram of cuprates, including the pseudogap phase, the strange metal phase, HTSC mechanism, variety of static and dynamic phase states. Numerous experimental data (see, for example, paper [1]), as well as a number of theoretical papers (see, for example, Hirsch's papers [2]), show the inapplicability of the concepts of the Bardeen–Cooper–Schrieffer (BCS) theory for HTSC cuprates. However, the inapplicability of the BCS theory to describe HTSC does not reduce the role of the electron-vibrational interaction in the formation of unusual properties of cuprates. Parent cuprates are characterized by very strong electron-lattice relaxation effects and proximity to a „polarization catastrophe" [3]. Direct quantum-chemical calculations [4] show that the electron-vibrational (vibronic) interaction leads to a significant renormalization of the adiabatic (thermal) charge transfer gap U_{th} compared to the optical gap U_{opt}, up to the possibility of its „overscreening" with a negative sign in parent cuprates with an ideal T'-structure [5]. As a result, the actual situation in doped cuprates with screened parameters of local and nonlocal correlations supposes the formation of a „boson-fermion" system of CuO_4-centers in CuO_2-planes, which can be in three charge

states of different valence close in energy: $[CuO_4]^{7-,6-,5-}$ (nominally $Cu^{1+,2+,3+}$), differing not only in charge, but also in an ordinary spin ($s = 0$ for $[CuO_4]^{7-,5-}$-centers and $s = 1/2$ for $[CuO_4]^{6-}$-center) and by orbital state (A_{1g} for $[CuO_4]^{7-,5-}$-centers and B_{1g} for $[CuO_4]^{6-}$-center) [6–13]. Following the spin-magnetic analogy proposed by Rice and Sneddon [14] to describe the three charge states (Bi^{3+}, Bi^{4+}, Bi^{5+}) of bismuth ion in $BaBi_{1-x}Pb_xO_3$, charge triplet $[CuO_4]^{7-,6-,5-}$ can be formally associated with the three states of the pseudospin $S = 1$ ($M = -1, 0, +1$, respectively), a spin-pseudospin („spin-charge") quartet of local states $|SMs\mu\rangle$ ($|10\frac{1}{2}\mu\rangle$, $|1-100\rangle$, $|1100]\rangle$) can be introduced, and traditional methods of spin algebra can be used for „non-quasi-particle" description of the system of strongly correlated many-electron centers with mixed valence in the „on-site" (CuO_4-cluster!) representation. Superconductivity in a system of charge triplets will be associated with the quantum transport of local composite bosons — pairs of holes localized on the CuO_4-cluster and described by a wave function with the symmetry $(d_{x^2-y^2})^2$ [13].

Recent discoveries of anomalous properties of cuprates and nickelates with the T'-structure [5,15], i.e., without apex oxygen, including the unexpected detection of HTSC in parent compositions, point to the important role of apex oxygen, but the headline is the need to refuse from the

generally accepted idea of the parent composition as an antiferromagnetic Mott–Hubbard insulator. Most likely, we should introduce a more universal definition of the „parent" system of planes CuO$_2$/NiO$_2$ with a nominal configuration 3d^9 for positions Cu/Ni, or „half filling", which, depending on the parameters of „out-of-plane" potential and electron-lattice relaxation, can be in various states, i.e., from antiferromagnetic or non-magnetic insulator, a Fermi metal to a high-temperature superconductor.

In this paper, within the framework of the previously proposed Hamiltonian of the charge triplet model [6–13] and the effective field theory, we consider the phase diagrams of CuO$_2$/NiO$_2$-planes, emphasizing the special role of the effect of phase separation and the formation of a nanoscopic phase-inhomogeneous structure. Using the classical Monte Carlo method and computer simulation, we discussed specific examples illustrating the structure of the phase inhomogeneous state in cuprates/nickelates with nonisovalent substitution.

2. Effective spin-pseudospin Hamiltonian

The spin algebra of (pseudo)spin systems with $S = 1$ ($M_S = 0, \pm 1$) includes eight independent operators (three dipole and five quadrupole):

$$S_z;\ S_\pm = \mp \frac{1}{\sqrt{2}}(S_x \pm iS_y);\ S_z^2:\ T_\pm = \{S_z, S_\pm\};\ S_\pm^2.$$

Instead of the raising/lowering operators $S_\pm$ and $T_\pm$ changing the pseudospin projection by ± 1, below we will use the combined operators

$$P_\pm = \frac{1}{2}(S_\pm + T_\pm);\ N_\pm = \frac{1}{2}(S_\pm - T_\pm),$$

more precisely, their generalization — the Fermi-type spin-pseudospin operators $\hat{P}_\pm^\nu$ and $\hat{N}_\pm^\nu$, which, taking into account the $s = 1/2$ spin state of [CuO$_4$]$^{6-}$-center ($|10\rangle$) change not only the local charge (pseudospin), but also spin states acting as follows on the spin-pseudospin quartet

$$\hat{P}_+^\nu \left|10; \frac{1}{2} - \nu \right\rangle = |11;00\rangle;\quad \hat{P}_-^\nu |11;00\rangle = \left|10; \frac{1}{2} - \nu\right\rangle;$$

$$\hat{N}_+^\nu |1-1;00\rangle = \left|10; \frac{1}{2}\nu\right\rangle; \hat{N}_-^\nu \left|10; \frac{1}{2}\nu\right\rangle = |1-1;00\rangle.$$

The operators $\hat{P}_\pm^\nu$ and $\hat{N}_\pm^\nu$ complying with anti-commutation relations describe the transitions [CuO$_4$]$^{6-}$ → [CuO$_4$]$^{5-}$ and [CuO$_4$]$^{6-}$ → [CuO$_4$]$^{7-}$ respectively, and are in fact the operators of creation/annihilation of electron/hole in the multielectron atomic state of the „parent" [CuO$_4$]$^{6-}$-center.

Purely pseudospin raising/lowering operators $S_\pm^2$ change the pseudospin projection by ± 2 and describe the transitions [CuO$_4$]$^{7-}$ ↔ [CuO$_4$]$^{5-}$, i.e., they are the creation/annihilation operators of the hole pair, or an effective

local composite boson. Average

$$\Psi = \langle S_\pm^2 \rangle = \frac{1}{2}\left(\langle S_x^2 \rangle - \langle S_y^2 \rangle \pm i \langle \{S_x, S_y\} \rangle\right)$$

can serve as a d-symmetric parameter of local superconducting order.

The complete set of local operators acting in the space of the spin-pseudospin quartet of CuO$_4$-center must also include the conventional spin operator of the „parent" [CuO$_4$]$^{6-}$-center.

The effective Hamiltonian of the system of charge triplets includes accounting of local and nonlocal correlations, three types of correlated single-particle transport, two-particle transport, Heisenberg spin exchange, and, generally speaking, electron-vibrational interaction. As for ordinary spin-magnetic systems, we can „integrate out" high-energy degrees of freedom and, after projecting onto a chosen local quartet $|SMs\mu\rangle$, taking into account spin algebra obtain the effective spin-pseudospin Hamiltonian CuO$_2$/NiO$_2$-plane of cuprate/nickelate in the form [6–13]

$$\hat{H} = \hat{H}_{\text{pot}} + \hat{H}_{\text{kin}}^{(1)} + \hat{H}_{\text{kin}}^{(2)} + \hat{H}_{\text{ex}}, \tag{1}$$

$$\hat{H}_{\text{pot}} = \sum_i (\Delta S_{iz}^2 - \mu S_{iz}) + \frac{1}{2}\sum_{i \neq j} V_{ij} S_{iz} S_{jz}, \tag{2}$$

$$\hat{H}_{\text{kin}}^{(1)} = -\sum_{i<j}\sum_\nu \Big[t_{ij}^p \hat{P}_{i+}^\nu \hat{P}_{j-}^\nu + t_{ij}^n \hat{N}_{i+}^\nu \hat{N}_{j-}^\nu$$
$$+ \frac{1}{2} t_{ij}^{pn}(\hat{P}_{i+}^\nu \hat{N}_{j-}^\nu + \hat{P}_{i-}^\nu \hat{N}_{j+}^\nu) + h.c. \Big], \tag{3}$$

$$\hat{H}_{\text{kin}}^{(2)} = -\sum_{i<j} t_{ij}^b (\hat{S}_{i+}^2 \hat{S}_{j-}^2 + \hat{S}_{i-}^2 \hat{S}_{j+}^2), \tag{4}$$

$$\hat{H}_{\text{ex}} = \frac{1}{4}\sum_{i<j} J_{ij} \boldsymbol{\sigma}_i \boldsymbol{\sigma}_j, \tag{5}$$

where $\boldsymbol{\sigma} = 2\hat{P}_0\mathbf{s}$, $\hat{P}_0 = 1 - \hat{S}_z^2$ is the operator of local spin density.

The spin-pseudospin Hamiltonian (1)−(5) contains only terms that do not change the total charge in the system, that is they preserve the z-component of the total pseudospin, which in ordinary spin-magnetic system would mean the preservation of z-component of magnetization. Naturally, the energy parameters in such Hamiltonian are effective variables that must be selected from comparison with experiment, or on the basis of estimates within the framework of one microscopic model or another.

The first term in (2) describes local correlation effects ($2\Delta = U$), in the second term μ — chemical potential, the last term in (2) describes nonlocal inter-site correlations. The Hamiltonian (3) describes three types of „single-particle" correlated transport, term (4) — „two-particle" transport, or the transport of composite bosons, term (5) — the Heisenberg exchange for parent [CuO$_4$]$^{6-}$-centers.

In the Hamiltonian (1) we actually limited ourselves by the approximation of „frozen lattice", whereas, strictly

speaking, this Hamiltonian should include not only the electron-vibrational interaction, but also the impurity potential in cuprates/nickelates with nonisovalent substitution, which generally plays an important role in the formation of inhomogeneous electronic state.

Introducing the „Cartesian" form of pseudospin operators [16]

$$\hat{S}_{\pm}^2 = \frac{1}{2}\left((\hat{S}_x^2 - \hat{S}_y^2) \pm i\{\hat{S}_x, \hat{S}_y\}\right) = \hat{B}_1 \pm i\hat{B}_2;$$

$$\hat{P}_{\pm}^\nu = \frac{1}{2}(\hat{P}_1^\nu \pm i\hat{P}_2^\nu); \quad \hat{N}_{\pm}^\nu = \frac{1}{2}(\hat{N}_1^\nu \pm i\hat{N}_2^\nu) \qquad (6)$$

with the Hermitian operators $\hat{B}_{1,2}$, $\hat{P}_{1,2}^\nu$, $\hat{N}_{1,2}^\nu$ we rewrite the spin-pseudospin Hamiltonian $\hat{H}$ in the equivalent „vector" form as

$$\mathscr{H} = \Delta \sum_i \hat{S}_{zi}^2 + V \sum_{\langle i,j \rangle} \hat{S}_{zi}\hat{S}_{zj} + Js^2 \sum_{\langle i,j \rangle} \hat{\boldsymbol{\sigma}}_i \hat{\boldsymbol{\sigma}}_j$$

$$- \mu \sum_i \hat{S}_{zi} - \frac{t_b}{2} \sum_{\langle ij \rangle} \hat{\mathbf{B}}_i \hat{\mathbf{B}}_j - \frac{t_p}{2} \sum_{\langle ij \rangle \nu} \hat{\mathbf{P}}_i^\nu \hat{\mathbf{P}}_j^\nu$$

$$- \frac{t_n}{2} \sum_{\langle ij \rangle \nu} \hat{\mathbf{N}}_i^\nu \hat{\mathbf{N}}_j^\nu - \frac{t_{pn}}{4} \sum_{\langle ij \rangle \nu} (\hat{\mathbf{P}}_i^\nu \hat{\mathbf{N}}_j^\nu + \hat{\mathbf{N}}_i^\nu \hat{\mathbf{P}}_j^\nu), \qquad (7)$$

where we limited ourselves considering the interaction of the nearest neighbors, $\hat{\boldsymbol{\sigma}} = (\hat{\sigma}_x, \hat{\sigma}_y, \hat{\sigma}_z)$, $\hat{\mathbf{B}} = (\hat{B}_1, \hat{B}_2)$, $\hat{\mathbf{P}}^\nu = (\hat{P}_1^\nu, \hat{P}_2^\nu)$, $\hat{\mathbf{N}}^\nu = (\hat{N}_1^\nu, \hat{N}_2^\nu)$.

Ignoring nonlocal correlations, that is, for $V_{ij} = 0$, the spin-pseudospin Hamiltonian of our model $(1)-(5)$ is formally equivalent to the sum of the Hamiltonians (7.8) and (7.15) from N. Plakida's book [17], written in terms of the Hubbard X-operators, but obtained within a rather controversial microscopic model $(U_d \to \infty, \dots)$. The Hamiltonian of local electron-vibrational (pseudospin-lattice) interaction with fundamental displacement modes of cluster CuO_4/NiO_4 of symmetry A_{1g}, B_{1g}, B_{2g} is presented in paper [13].

3. Phase states and phase diagrams of the charge triplet model

The rather complex structure of the local Hilbert space (quartet!) with a large number of local order parameters and effective spin-pseudospin Hamiltonian $(1)-(5)$ or (7) point to a large number of possible phase states of the „charge triplet" model. One or another long-range order in the system, which is established with temperature decreasing, is the result of competition and evolution of the short-range order formed by the main intercenter interactions. Thus, in the nearest neighbors approximation the exchange interaction is primarily responsible for the formation of spin-antiferromagnetic dielectric phase (AFMI) with a local parameter $\langle \sigma \rangle$, nonlocal correlations (V) — for the staggered-type charge ordering (CO, or CDW with

$\mathbf{q} = (\pi, \pi)$) with local „pseudo-antiferromagnetic" parameter $L_z = \langle S_{zA} \rangle - \langle S_{zB} \rangle$, two-particle transfer — for phase of bosonic superconductivity (dBS) with d-symmetric order parameter $\langle S_{\pm}^2 \rangle$, single-particle transfer — for two coherent Fermi-type metallic phases, hole (P) and electron (N), characterized by local parameters $\langle P_{\pm}^\sigma \rangle$ and $\langle N_{\pm}^\sigma \rangle$ respectively [13]. Note that local average of fermionic operators of $\langle P_{\pm}^\nu \rangle$ and $\langle N_{\pm}^\nu \rangle$ types were first used in the mean field approximation by Caron and Pratt [18]) to describe the Hubbard model in real-space, rather than k-momentum, as usual, representation. Metallic P- and N-states interact and mix due to PN (NP) contributions to single-particle transport (3), which leads to unusual properties of metal phases of cuprates/nickelates with specific coexistence of electron and hole carriers in cuprates with both hole and electron doping [19,20]. Here we mentioned the simplest „monophases" with a single non-zero local order parameter. But remember that these phases of the „Neel" type are just some classical limit of the actual quantum phases of the ground state, the manifestation of which we see, in particular, in the effect of „quantum" reduction of the value of the local order parameter, which is well known for quantum magnetics. However, along with semiclassical phases of the „Neel" type in the CuO_2/NiO_2 planes of cuprate/nickelate it is possible to form a purely quantum nonmagnetic dielectric phase as a system of quantum electron-hole (EH) dimers of the Anderson RVB-phase type, the stability of which will be maintained due to the effects of electron-lattice relaxation [11].

The spin-pseudospin structure of the effective Hamiltonian makes it possible to use for the analysis of phase states and phase diagrams of the charge triplets model the methods well known for typical spin-magnetic systems, primarily the effective field method, which makes it possible to accurately consider local correlations, and all inter-site interactions within the molecular field approximation (MFA) typical for spin-magnetic systems [12,13,21]. The simple theory of the effective or mean field in the usual real-space representation is, as always, a good starting point for a physically clear semiquantitative description of strongly correlated electron systems, primarily spin or pseudospin systems.

The semiclassical phase states of the complete model of charge triplets in the framework of the effective field approximation were recently analyzed in papers [12,13] with the subsequent Maxwell's construction, which allows one to numerically find the boundaries of the phase separation regions, in particular, the lines of phase transitions of the „third order" and to plot phase diagrams of CuO_2/NiO_2-plane („2D diagrams") for various energy parameters of the model, at this point not considering their dependence on the degree of doping. Fig. 1 (top panel) shows several options of „single-phase" diagrams for the CuO_2/NiO_2 planes obtained in the framework of the two-sublattice model with nearest neighbors interaction. The phases corresponding to the free energy minimum are marked with different colors.
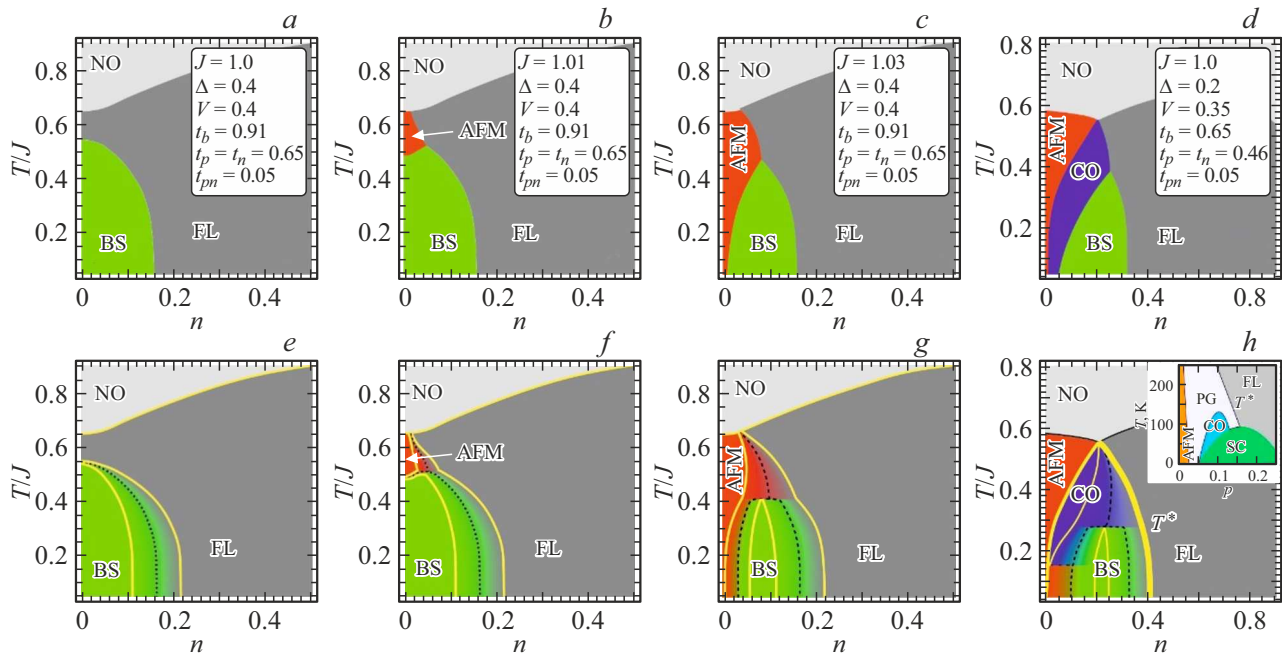
Figure 1. Model 2D $T-n$-phase diagram of cuprate/nickelate with hole doping $(n = p)$ assuming implementation of „monophases" NO, AFMI, BS, FL, CO, calculated in the effective field approximation at constant values of the Hamiltonian parameters (see text). Top panel — phase diagrams without taking into account the possible coexistence of „adjacent" phases; bottom panel — phase diagrams considering phase separation. Black dotted and solid curves are lines of phase transitions of the first and second order, respectively, dashed lines in the diagrams of the bottom panel indicate the boundary of regions with the same volume fraction of coexisting phases, yellow curves indicate the lines of phase transitions of the „third" order, i.e., the boundaries of areas with 100% volume fraction. The inset in the diagram h is a typical phase diagram of a cuprate with hole doping.

The phase diagram shown in Fig. 1, a was calculated for rather arbitrarily chosen model parameters (see inset), whose ratio is characterized by the complete suppression of the AFMI and CO phases in favor of the BS and FL phases, which form the ground state of the CuO_2/NiO_2 planes at $0 \le n \le 0.16$ and $n > 0.16$, respectively. Such phase diagrams without signs of long-range order AFMI and CO turn out to be typical for cuprates with an ideal or almost ideal T'-structure [5], and, possibly, nickelates, the structure of which also has no apex oxygen [15]. However, for the chosen energy parameters the free energies of the phases AFMI and BS turn out to be close, so that the exchange integral increasing by 1% only leads to the appearance of AFMI phase initially in a small section of the phase diagram (Fig. 1, b), and with increasing by 3%, the AFMI phase forms the ground state of the system in the region of low doping concentrations (Fig. 1, c). With the local correlation parameter decreasing by two times the system exhibits a step-by-step AFMI-CO-BS-FL transformation of the ground state with phase diagram typical for many hole-doped cuprates (Fig. 1, d).

However, ordered homogeneous phases turn out to be unstable with respect to phase separation (PS). As a result of the numerical implementation of the Maxwell construction [21–23] with the same parameters of the model Hamiltonian as above, we found that phase separation is indeed observed in the region of coexistence of phases

AFMI-FL, AFMI-BS, CO-BS, CO-FL, and BS-FL, separated by first-order phase transition lines, but absent in the region of coexistence of AFMI-CO phases. The coexistence of the AFMI and CO phases means the possibility of the formation of a homogeneous mixed phase, such as the spin-charge (spin-pseudospin) density wave, although, most likely, effects characteristic for the region of coexistence of the corresponding „monophases" will also be observed. The phase diagram for our model cuprate, plotted considering the phase separation and presented in the bottom panel of Fig. 1, differs significantly from the „naive" phase diagram (top panel of Fig. 1), obtained without phase separation. The lines of phase transitions of the „third" order, i.e., the boundaries of regions with 100% volume fraction are highlighted in yellow on the bottom panel, dashed lines indicate the boundaries of regions with the same volume fraction of coexisting „monophases". The specific shape of the domains in PS-state is determined, in particular, by the long-range Coulomb interaction and the surface energy, i.e., the energy of the interfaces.

The conclusion about the „global" nature of the electronic phases separation in the CuO_2 planes is of fundamental importance both in general for understanding the physics of the normal and superconducting states of cuprates, and in particular for explaining the HTSC mechanism itself. Thus, following the authors of paper [24], we can say that the superconductivity of cuprates is not directly related to the

pairing of doped holes or electrons. Doped carriers only form a normal metallic FL-phase. The superconducting state of cuprates with d-symmetry of the order parameter is formed by „hole" local composite bosons having $d_{x^2-y^2}^2$ symmetry. Formally, all „monophases", i.e., AFMI, CO, BS, and FL, are possible phase states of parent cuprates; while if for cuprates with T- structure the AFMI-phase is the ground state, then for curpates with ideal T'-structure the ground state is formed by superconducting BS-phase [5,25].

The superconducting transition in the PS-state will have a two-step nature with the formation at $T > T_c$ of isolated BS-domains without phase coherence and the subsequent percolation transition with phase-synchronization of BS-domains due to the Josephson interaction at a lower temperature T_c, when the Josephson coupling between BS-domains is approximately equal to the thermal energy.

A tendency to phase separation as a universal feature of doped cuprates is evidenced by a large number of experimental facts (see, for example, papers [24,26–28] and references therein). Thus, the coexistence of normal phase regions with a superconducting condensate agrees with the measurements of excess thermal conductivity and heat capacity [20]. Unfortunately, despite these evidences, most theoretical approaches to describing the normal and superconducting states of cuprates are based on the assumption of homogeneous phases.

All AFMI, CO, and BS „monophases" characterized by the presence of specific energy gaps, are separated from the 100% coherent metallic Fermi-liquid FL-phase by a phase transition line of „third order" $T^*(p)$, which is the main candidate for the „pseudogap" temperature, which determines the boundary of the „pseudogap" phase. The actual inhomogeneous electronic structure of the pseudogap phase is determined by the complex competition of the Nèel-type „monophases" with non-zero local order parameters and quantum phases of the type of electron-hole dimers system [11].

The PS-model predicts the appearance of several characteristic temperatures of percolation transitions inside the pseudogap phase, which will manifest themselves in the features of the temperature behavior of various thermodynamic quantities [29].

4. Computer simulation of phase heterogeneity in CuO₂/NiO₂ planes of cuprates/nickelates

Maxwell's effective field theory and construction give only semi-quantitative information on the position of phase separation regions and volume fractions of phases depending on the temperature and degree of doping, but they do not provide any information on the actual structure of the phase-inhomogeneous state, which, most likely, will be determined by such factors as defectiveness, size and shape of the sample. Below, for illustration, we discuss several particular variants of the complete model of charge

triplets. The analysis of particular variants such as the atomic limit, the limit of large negative U, „spinless" limit, within the framework of the molecular field approximation and the Maxwell construction, classical and quantum Monte Carlo, allows us to demonstrate the formation and features of phases separation, the structure of domain boundaries, which, as a rule, are the centers of formation of new phase-heterogeneous states.

4.1. Atomic limit

The atomic limit, in which we neglect both one- and two-particle transport, was discussed by us in sufficient details in a series of papers [30–35] in the framework of a simplified two-sublattice model and the Ising exchange interaction using the molecular field approximation, the Bethe cluster model and the classical Monte Carlo method. For illustration, Fig. 2 shows in the strong exchange limit the calculated phase $T-\Delta$ (Fig. 2,a) and $T-n$ (Fig. 2, bottom panel) diagrams, as well as the specific heat capacity vs. temperature (Fig. 2,b). Both the molecular field approximation and the Monte Carlo method indicate a low-temperature phase transition of the „third order" to the PS-state with the phase separation AFMI-CO. The bottom panel of Fig. 2 shows examples of the structure of PS-state in the region of small („CO-droplets" in the AFMI-matrix) and large („AFMI-droplets" in CO-matrix) of doping concentrations obtained from the Monte Carlo calculations.

4.2. Limit of large negative $U = 2\Delta$

In the limit of large negative $U = 2\Delta \rightarrow -\infty$, the local Hilbert space is reduced to the pseudospin doublet $M_S = \pm 1$, and the system of charge triplets is reduced to the system of electron and hole centers, which is equivalent to the well-known system of local (hard-core) bosons [36], which, depending on the model parameters (t_b and V), can be found in the ordered states CO and BS. Obviously, the study of the competition between superconductivity and charge ordering is of particular interest for HTSC cuprates. We used high-performance parallel computing on NVIDIA graphic cards using the nonlinear conjugate gradient method and the Monte Carlo method to directly observe the formation of the ground state configuration of a two-dimensional system of local bosons with temperature decreasing and its evolution with a deviation from half-filling [37,38]. Systematic studies on large square lattices shown that in the absence of doping ($n = 0$) the temperature decreasing leads to the formation of both a stable homogeneous CO-phase and a relatively stable domain structure of CO-phase with a stripe-like domain boundaries, oriented predominantly along the principal axes of the lattice. Antiphase domain boundaries in the CO-phase are in fact the regions of „filamentary" superconductivity [37,38], at that along with a simple uniform („ferromagnetic") phase distribution of the order parameter of BS phases
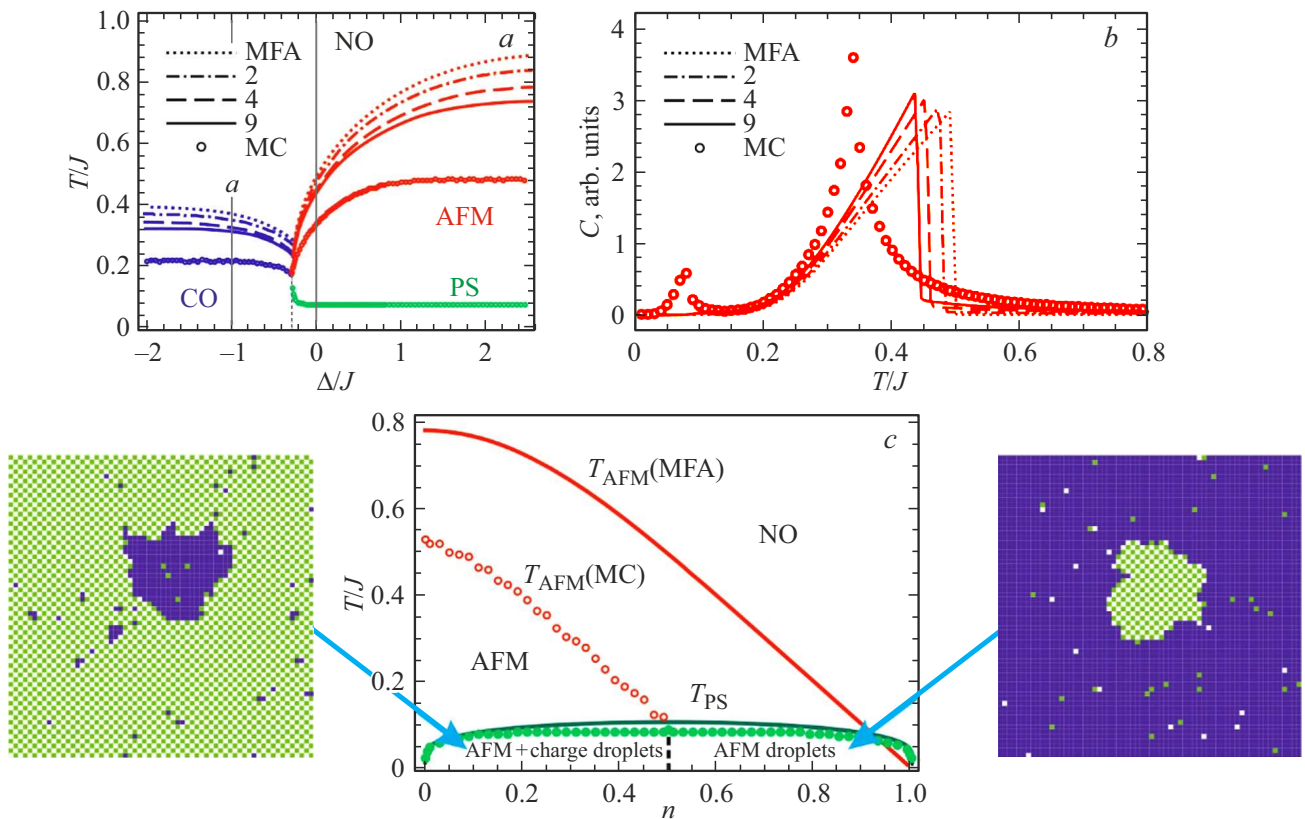
Figure 2. Top panel (*a*): phase $T-D$-diagram for the atomic limit at $n = 0.1$, $J = 0.25$, $V = 0.1$ obtained using MFA models, Bethe cluster models and calculations by the classical Monte Carlo method. Top panel (*b*): specific heat vs. temperature obtained using the MFA models, Bethe cluster models and classical Monte Carlo calculations. Bottom panel: $T-n$ phase diagram in the strong exchange limit. The open circles point to the Monte Carlo results for the susceptibility maxima at the AFM ordering and the solid circles point to the heat capacity maxima at the PS-transition. The solid lines show the critical temperatures T_{AFM} and T_{PS} calculated in the mean field approximation.
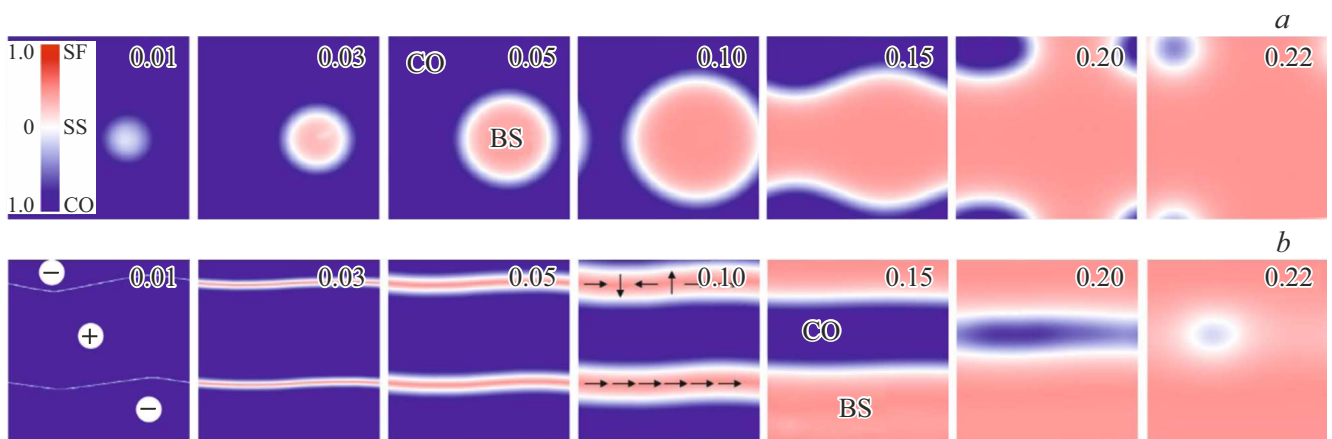

Figure 3. Two scenarios of the ground state configuration evolution for the hc-bosons system with doping increasing in the region of phases separation. In the top right corners of the individual panels the half-filling deviation n is indicated. *a*) Nucleation and growth of topological defects (droplets) that can accommodate all doped bosons. *b*) Broadening of the domain boundaries of the stripe-like CO phase and the appearance of a filamentary BS phase in them due to the doped bosons localization inside the domain boundaries. Signs „plus" and „minus" indicate different CO-domains. With a well-defined phases separation, systems of almost parallel domains of the CO and SF phases arise, separated by domain boundaries of a „supersolid" phase. The orientation of the phase angle φ inside the domain walls is shown schematically for $n = 0.1$.
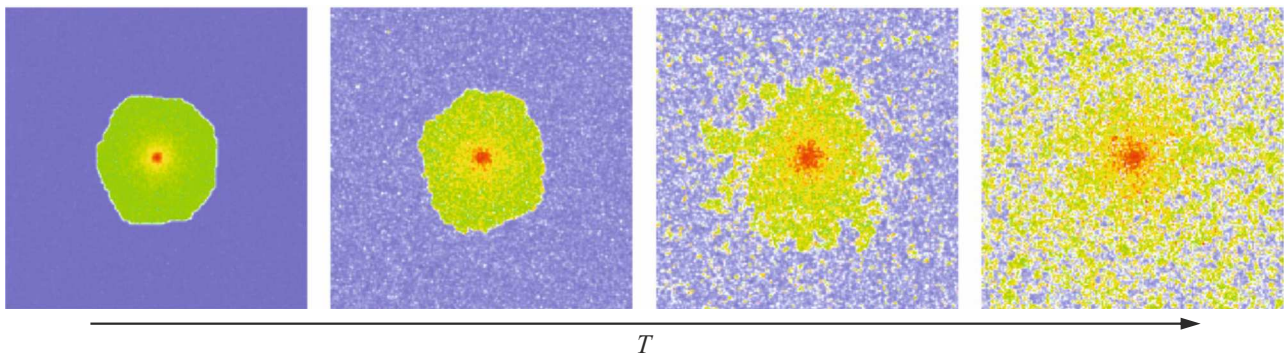
Figure 4. Illustration of the cylindrical domain formation of the superconducting BS-phase at the „out-of-plane" impurity potential in the parent cuprate/nickelate with the ground AFMI state.

at the center of the boundary they can have an unusual multidomain topological structure with a high density of 2π-boundaries separating one-dimensional phase domains. The evolution of both homogeneous and stripe-like configurations of the ground state of the system of local bosons under doping is shown in Fig. 3, a, b. For the initial homogeneous state, a small deviation from half-filling at $n \leq 0.01$ practically does not lead to visible effects, slightly breaking the residual heterogeneity. However, at $n \approx 0.01$ there is a sudden formation of rather large topological defects (droplets), which are mainly cylindrical in shape and consist of BS-core and a ring-shaped boundary with the „supersolid" phase structure [36]. These droplets could accommodate all the doped bosons, preserving the uniform surrounding CO-phase. When doping increases, we come to a well-defined phases separation with an increasing volume fraction of large defects, with a change in their shape and their merging up to a complete phase transition CO-BS near the critical value $n_{cr} \approx 0.22$. The evolution of the stripe-like CO-phase with filamentary superfluidity, when deviating from half-filling, proceeds according to a different scenario, since doped bosons are localized at the center of narrow domain walls, which leads to their uniform broadening up to the formation of BS-phase domains. It is notable that the structure of the final BS-phase in this case depends on the initial topological structure of the phase parameter of BS-phase (φ) in one-dimensional domain boundaries. Fig. 3, b shows the option of the initial state with two one-dimensional domain walls with a uniform distribution of the phase parameter of BS-phase for the bottom wall and with 2π-domain boundary separating one-dimensional phase domains for the top wall. The phase angle φ orientation inside the domain walls is schematically shown in Fig. 3, b for $n = 0.1$. Upon deviation from half-filling in a well-defined phases separation regime, we get a system of almost parallel domains of CO- and SF-phases separated by domain walls with the „supersolid" phase structure. However, the regular domain structure becomes more and more unstable up to the limiting doping concentrations with the formation of BS-phase with topological defects. Note that in both cases considered, the phases separation is

formed more likely according to the scenario typical for the first-order phase transitions in systems with nuclei of the „new" phase.

4.3. Features of the formation of phase-inhomogeneous states in cuprates/nickelates with nonisovalent substitution

It is obvious that both the 2D phase diagrams and especially the 3D diagrams of actual bulk cuprates/nickelates with „nonisovalent" substitution ($La_{2-x}Sr_xCuO_4$, $YBa_2Cu_3O_{6+x}$, ...) will be significantly modified taking into account the impurity „out-of-plane" Coulomb potential as some „external" initiator of electronic inhomogeneity.

Preliminary model calculations carried out by us by the classical Monte Carlo method on large square lattices show the possibility of the formation of local superconductivity regions near such impurities even in the initial antiferromagnetic dielectric matrix. Fig. 4 illustrates the formation/destruction of the cylindrical domain of BS-phase upon the temperature decreasing/increasing in the „parent" antiferromagnetic CuO_2 — plane of the model cuprate of type $La_{2-x}Sr_xCuO_4$ taking into account the „out-of-plane" Coulomb potential created by a separate Sr^{2+} ion. For simplicity, we neglected single-particle transport, assuming $t_p = t_n = t_{pn} = 0$. The choice of the remaining model parameters: $J = 1$, $V = 0.1$, $\Delta = 0.02$, $t_b = 0.55$ corresponded to the ground AFMI state of the CuO_2-plane in the absence of an impurity potential.

Nonisovalent impurities can serve as pinning centers for various topological defects such as skyrmions or cylindrical domains (bubbles) [8], as well as domain boundaries. Fig. 5 illustrates the process of evolution of the branched domain structure of the CO-phase of charge triplets system with parameters $J = 1$, $V = 0.3$, $\Delta = 0.02$, $t_b = 0.55$, $t_p = t_n = t_{pn} = 0$ in the presence of the „out-of-plane" Coulomb potential. The process of gradual „freezing" of domain boundaries with temperature decreasing stops when the nearest domain boundary is pinned at the
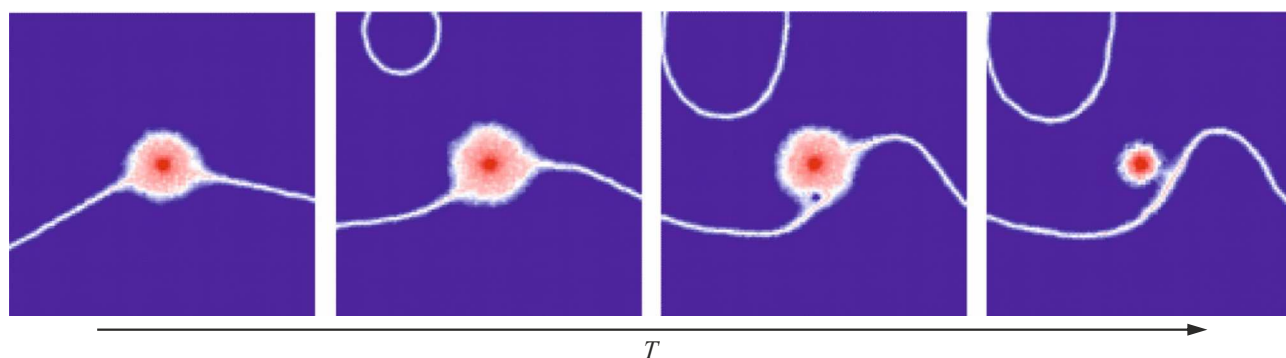
Figure 5. Illustration of CO-phase domain wall pinning at the „out-of-plane" impurity potential in the parent cuprate/nickelate with the ground CO-state.

impurity potential. Note that the domain boundaries of the CO-phase represent regions of the filamentary BS-phase (superconductivity), and the region at the center of the impurity potential is the cylindrical domain of the BS-phase.

5. Conclusion

We develop a scenario for the formation of the electronic structure of HTSC of cuprates/nickelates, which is based on the description of the charge degree of freedom of the CuO_2/NiO_2-planes within the „non-quasiparticle" model of charge triplets — clusters of the type $[CuO_4]^{7-,6-,5-}$ (nominally $Cu^{1+,2+,3+}$-centers) in cuprates using the $S = 1$ pseudospin formalism. The effective spin-pseudospin Hamiltonian, which takes into account the main local and nonlocal correlations, single- and two-particle transport, and spin exchange, makes it possible to use all methods of analysis well known for spin-magnetic systems, in particular, the effective field theory with the exact consideration of local correlations and the molecular field approximation to take into account inter-site interactions.

The ground state of parent systems can be not only an antiferromagnetic insulator (AFMI), but also a bosonic superconductor (BS), a nonmagnetic charge-ordered insulator (CO), an unusual Fermi metal, and also a quantum insulator like a system of electron-hole dimers. The typical state of doped cuprate/nickelate, in particular a „mysterious" pseudogap phase, is the result of phases separation. The superconductivity of cuprates/nickelates is not a consequence of the pairing of doped holes or electrons, but is the result of the condensation of hole composite bosons, while the main features of the normal state can be associated both with the electron-hole nature of the unusual Fermi liquid phase and with the features of phases separation. The global nature of the electronic phases separation in the CuO_2/NiO_2-planes makes it possible to understand and explain many fundamental features of the physics of the normal and superconducting states of cuprates/nickelates, including the formation mechanism of the HTS and pseudogap phase.

On a number of particular examples of the implementation of the model of charge triplets in the framework of the classical Monte Carlo method, we considered the features of phase inhomogeneous states and their evolution with changes in temperature and doping degree, including the special role of the impurity potential in cuprates/nickelates with nonisovalent substitution.

Conflict of interest

The authors declare that they have no conflict of interest.

References

[1] X. Bozovic, J. He, A. Wu, T. Bollinger. Nature **536**, 309 (2016).
[2] J.E. Hirsch. Physica Scripta, **80**, *3*, 035702 (2009).
[3] B.P.P. Mallett, T. Wolf, E. Gilioli, F. Licci, G.V.M. Williams, A.B. Kaiser, N. Suresh, J.L. Tallon, N.W. Ashcroft. Phys. Rev. Lett. **111**, 237001 (2013).
[4] S. Larsson. Physica C **460-462**, 1063 (2007).
[5] M. Naito, Y. Krockenberger, A. Ikeda, H. Yamamoto. Physica C **523**, 28 (2016).
[6] A.S. Moskvin. Phys. Rev. B **84**, 075116 (2011).
[7] A.S. Moskvin. J. Phys.: Condens. Matter **25**, 085601 (2013).
[8] A.S. Moskvin, Y.D. Panov. J. Supercond. Nov. Magn. **32**, 61 (2019).
[9] A.S. Moskvin, Yu.D. Panov. FTT **61**, 1603 (2019) (in Russian).
[10] A.S. Moskvin. Phys. Met. Metallogr. **120**, 1252 (2019).
[11] A.S. Moskvin, Y.D. Panov. Phys. Solid State **62**, 1554 (2020).
[12] A.S. Moskvin, Y.D. Panov. Condens. Matter, **6**, 24 (2021).
[13] A.S. Moskvin, Y.D. Panov. JMMM **6**, 24 (2022).
[14] T.M. Rice, L. Sneddon. Phys. Rev. Lett. **47**, 689 (1981).
[15] D. Li, K. Lee, B.Y. Wang et al. Nature (London), **572**, 624 (2019).
[16] Yu.D. Panov. Phys. Metals Metallogr. **120**, 1276 (2019).

[17] Nikolay M. Plakida. High-Temperature Cuprate Superconductors. Experiment, Theory, and Applications, Springer, Berli–Heidelberg–N. Y.–Hong Kong–London Milan–Paris–Tokyo 2011.

[18] L.G. Caron, G.W. Pratt. Rev. Mod. Phys. **40**, 802 (1968).

[19] N. Luo, G.H. Miley. J. Phys. Condens. Matter **21**, 025701 (2009).

[20] D.R. Harshman, J.D. Dow, A.T. Fiory. Phil. Mag. **91**, 818 (2011).

[21] K. Kapcia, S. Robaszkiewicz, R. Micnas. J. Phys.: Condens. Matter **24**, 215601 (2012).

[22] E. Arrigoni, G.C. Strinati. Phys. Rev. B **44**, 7455 (1991).

[23] A.L. Rakhmanov, K.I. Kugel, A.O. Sboychakov. J. Supercond Nov. Magn. **33**, 2405 (2020).

[24] D. Pelc, P. Popcevic, M. Pozek, M. Greven, N. Bariusic. Sci. Adv. **5** eaau4538 (2019).

[25] T. Adachi, T. Kawamata, Y. Koike. Condens. Matter, **2**, 23 (2017).

[26] V.Z. Kresin, Yu.N. Ovchinnikov, S.A. Wolf. Phys. Rep. **431**, 231 (2006).

[27] E.V.L. de Mello, E.S. Caixeiro. Phys. Rev. B **70**, 224517 (2004).

[28] E.M. Motoyama G. Yu, I.M. Vishik, O.P. Vajk, P.K. Mang, M. Greven. Nature **445**, 186 (2007).

[29] V. Sacksteder. J. Supercond. Nov. Magn. **33**, 43 (2020).

[30] Yu.D. Panov, K.S. Budrin, A.A. Chikov, A.S. Moskvin. JETP Lett. **106**, 242 (2017).

[31] Y.D. Panov, A.S. Moskvin, A.A. Chikov, K.S. Budrin. J. Low Temp. Phys. **187**, 646 (2017).

[32] A.A. Chikov, Y.D. Panov, A.S. Moskvin, K.S. Budrin. Acta. Phys. Pol. A **133**, 432 (2018).

[33] Y.D. Panov, V.A. Ulitko, K.S. Budrin, A.A. Chikov, A.S. Moskvin. J. Magn. Magn. Mater. **477**, 162 (2019).

[34] Y.D. Panov, K.S. Budrin, V.A. Ulitko, A.A. Chikov, A.S. Moskvin. J. Supercond. Nov. Magn. **32**, 1831 (2019).

[35] Yu.D. Panov, A.S. Moskvin, V.A. Ulitko, A.A. Chikov. FTT **61**, 1676 (2019) (in Russian).

[36] R. Micnas, J. Ranninger, S. Robaszkiewicz. Rev. Mod. Phys. **62**, 113 (1990).

[37] A.S. Moskvin, Y.D. Panov, F.N. Rybakov, A.B. Borisov. J. Supercond. Nov. Magn. **30**, 43 (2017).

[38] A.S. Moskvin, Yu.D. Panov, F.N. Rybakov, A.B. Borisov. FTT **59**, 2107 (2017) (in Russian).